СООБЩЕНИЯ
ОБЪЕДИНЕННОГО
ИНСТИТУТА
ЯДЕРНЫХ
ИССЛЕДОВАНИЙ

Дубна

E1-98-192

V.Yu.Alexakhin, N.A.Kuchinsky, E.A.Pasyuk,
M.G.Sapozhnikov

SIMULATION OF THE FIRST MUON FILTER FOR THE COMPASS SPECTROMETER

1998

1 Introduction

The COMPASS spectrometer is under construction at the M2 beam channel of SPS (CERN) in a framework of NA-58 experiment [1]. The purpose of this experiment is to study the hadron structure and spectroscopy with high intensity muon and hadron beams. A distinct feature of the COMPASS programme will be the collection of high statistics samples of charmed particles. From a measurement of the cross-section asymmetry for open charm production in deep inelastic scattering of polarized muons on polarized nucleons it is planned to determine the gluon polarization ΔG. Using hadron beams is planned to study semi-leptonic decays of charmed baryons as well as doubly charmed baryons. Meson spectroscopy and the search for exotic states (like glueballs and hybrids) are also included in the COMPASS physical programme. To pursue these physics objectives, a new spectrometer is proposed with excellent particle identification and calorimetry able to operate at beam intensities up to $2 \cdot 10^8$ particles/spill.

The COMPASS experimental setup consists of two spectrometers - Large Angle Spectrometer (LAS) and Small Angle Spectrometer (SAS). The design of the spectrometers is similar and comprises (along the beam) a magnet, SM1/2, a ring imaging Cherenkov counter, RICH1/2, an electromagnetic calorimeter, ECAL1/2, a hadron calorimeter, HCAL1/2 and finally, a muon filter, μF1/2, where 1 and 2 refer to the LAS and SAS, respectively. The layout of LAS is shown in Fig. 1.

The JINR physicists are in charge of the construction of the hadron calorimeter HCAL1 and the First Muon Filter (μF1). The goal of this report is to summarize the results of the Monte Carlo simulation of the First Muon Filter.

The muon filter serves to identify and detect the scattered muon in the muon programme and muons from the semi-leptonic decays of charmed baryons in the hadron programme. The muons from D_s and J/ψ muonic decays are also detectable. The μF1 is mainly needed to detect the muons scattered at large angles.

2 First Muon Filter Layout

The μF1 consists of 4 muon stations (MST1-MST4). The first two muon stations should be placed downstream of the hadron calorimeter, HCAL1 (Fig.1), followed by 1 m of iron and two more muon stations. There is the hodoscope mHOD1, upstream of muon station MST1 which should provide the muon trigger. A similar hodoscope, mHOD2, is located in front of MST3. In the simulation the dimension of mHOD1 is 400×300 cm^2 with a hole of 172×92 cm^2 around the beam. The corresponding dimension of mHOD2 is 500×400 cm^2 with the same hole.

Each muon station consists of X and Y planes (Fig. 2), each plane consists of 2 layers of aluminium mini-drift tubes (MDT) [2] staggered by 0.5 cm to increase detector efficiency. The design of a drift tube is shown in Fig. 3. The tubes are operating in the proportional mode to obtain high rate capabilities of up to 10^5 particles per wire.

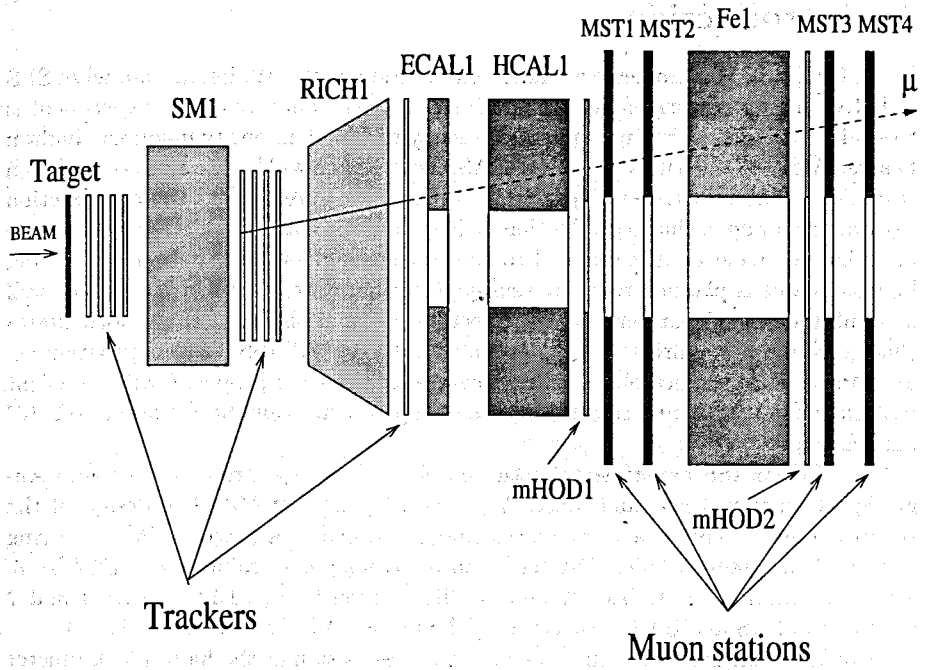

Figure 1: The Large Angle Spectrometer of the COMPASS setup.

The main task of μF1 is to identify the muon and match its track with the signals given by the tracking chambers downstream the HCAL1.

The muon identification is based on high penetrability of muons, which allows them to pass through the hadron calorimeter HCAL1 with effective thickness of $\sim$ 1 m of iron and the muon absorber which is also 1 m of iron.

The multiple scattering (MS) of low energy muons in the absorber is quite large (about 12 mrad for 10 GeV muons), thus, the requirements to the detector resolution are modest. The spatial resolution needed to match the effect from the MS in the iron is about 5 mm. In addition MS in the hadron calorimeter should be considerd because it is relevant to match the downstream muon track with the upstream one. Assuming the MS in calorimeter to be again about 12 mrad at 10 GeV, we arrive at a needed spatial resolution of about 0.5-1 cm.

3 Simulation of the muon detection efficiency

The muon detection efficiency with respect to the trigger hodoscopes mHOD1 and mHOD2 (see Fig. 1) was estimated using two options of the tube design:
a) 8 rectangular gas cells with 9×9 mm^2 cross section in case of plastic profile,

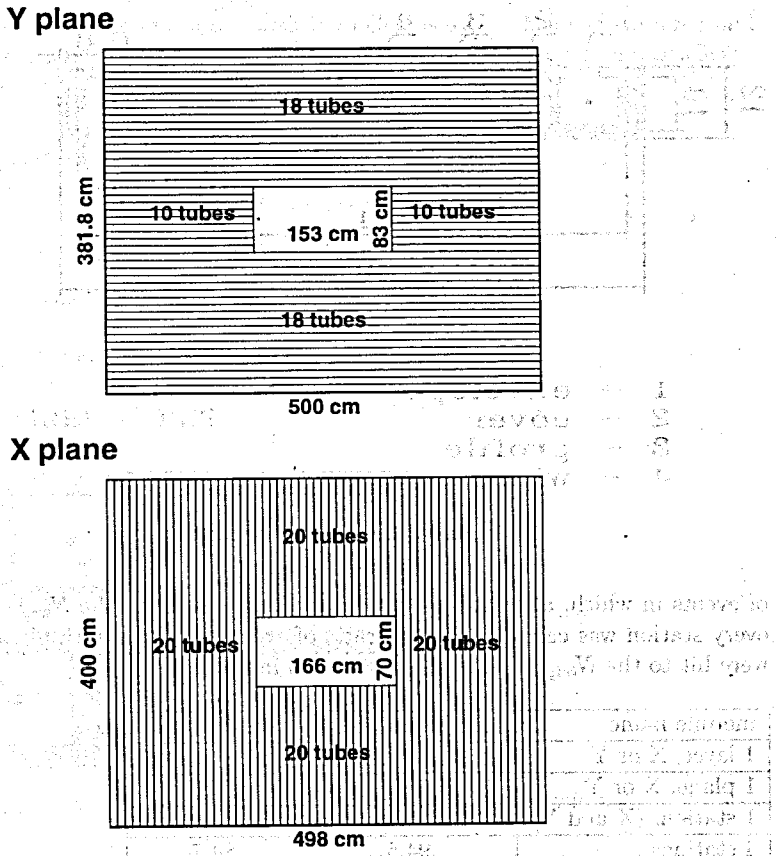

Figure 2: Design of the X and Y planes.

b) 9.2×9.2 mm^2 in case of aluminium profile,
inserted in the plastic envelope with the cross section of 13×85 mm^2 (plastic profile) or 12.1×83 mm^2 (aluminium profile).

The length of gas cells is by 12 cm shorter than the tube length in order to imitate the endcup region of the tube. Inside each cell a 2.5-cm-long dead zones were placed with 50 cm steps, to imitate the wire support and the insensitive zone around it. We considered a cell to be active if energy deposition in it was greater than 1 keV (with $CF_4(90\,\%) + CH_4(10\,\%)$ gas mixture). The distribution of muons within the solid angle was assumed to be uniform.

The efficiency of a layer was calculated as an average number of hits in X and Y layers, divided by number of trigger events N_{trig}. The hits in mHOD1 and mHOD2 were assumed as a trigger. Efficiency of a plane was calculated as a ratio of number

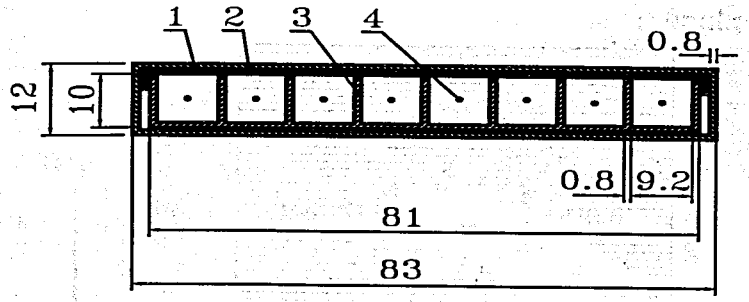

1 – envelope
2 – cover
3 – profile
4 – wires

Figure 3: Design of the drift tube.

of events in which, at least, one layer in a plane was hit to the N_{trig} . Efficiency of every station was calculated as the ratio of events in which both planes (X and Y) were hit to the N_{trig}. The results are shown in Table 1.

module name	aluminium profile	plastic profile
1 layer, X or Y	88.2	84.2
1 plane, X or Y	99.3	97.9
1 station, (X and Y)	98.6	95.9
4 stations	94.5	84.7

Table 1: Efficiency of muon registration in %. Statistical errors are about 0.2%.

The efficiency of the station given in the Table 1 leads to 94.5 % efficiency if the hits in all 4 stations are required for the aluminium profile and 84.7 % for the plastic one. Therefore, the aluminium profile 0.8 mm thick gives a 10 % gain in overall efficiency to be compared to the 1 mm thick plastic profile.

4 Simulation of the muon identification

The expected particle flux in μF1 planes region is up to 300 Hz/cm^2 (muon halo) in case of the muon beam. This leads to an average amount of background particles <N>=12 passing through the planes of μF1 during 200 ns (time gate). A large amount of material (about 115 X_0) along the muon trajectory leads to a strong multiple scattering for muons with momentum less than 10 GeV. Mean square deviation

σ from the initial direction for muons with P=5 GeV is σ_{Y1}=5.5 cm at station 1 and σ_{Y3}=11 cm at station 3. This leads to a high probability of background particles to imitate the muon track.

4.1 Detector options

We have considered three options of the detector:

- standard, without strips (Fig. 3)
- with paired wires of adjacent layers (Fig. 4)
- standard, with strips between layers

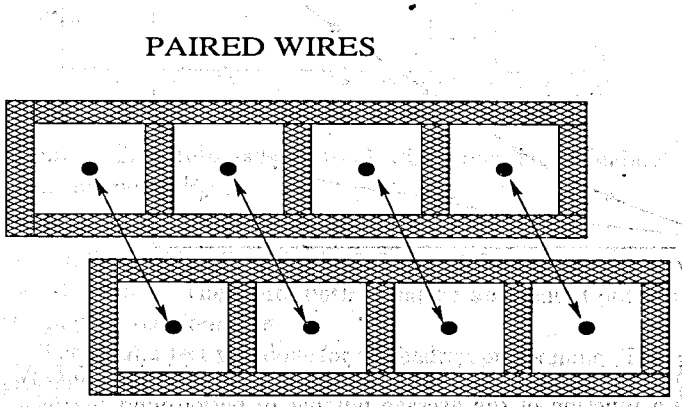

Figure 4: Schematical representation of the paired wires.

Pairing of wires means that two wires from adjacent layers are coupled to one electronic channel.

The option with strips should provide a better track identification. We assume that the strip width is 1 cm and the strips are inclined at 45 degrees with respect to the wires. One particle fires 3-5 strips and the amplitude from the strips was not assumed to be measured.

To compare different detector options, it was assumed that the muon halo is the only source of the background. The probability of misidentification W was determined as follows. The momentum of the muon was chosen to be 5 GeV/c, it is most probable momentum for muons from $D_s \to \mu^- \nu$ decays. The random directions of the muon were simulated. The tracking stations downstream the HCAL1 give information about the direction of the muon. Knowing the coordinates X_0, Y_0 in the muon stations and the dispersion due to the multiple scattering $\sigma_{X(Y)}$, we have checked if there are any hits from the muon halo within the range of $X_0(Y_0) \pm 3\sigma_{X(Y)}$.

In case of the option with strips the value $V(X,Y) = \frac{1}{\sqrt{2}}(X+Y)$ for a certain station was compared with known exact value V_0 for all hits of this station. If the

absolute value of difference $\Delta V = V_0 - V(X,Y)$ is less than 3 cm (for a combination of hits (X,Y)), this combination is used for the identification.

The probabilities W for different average numbers of background particles <N> are shown in Fig. 5 for different options of the detectors. One can see that the

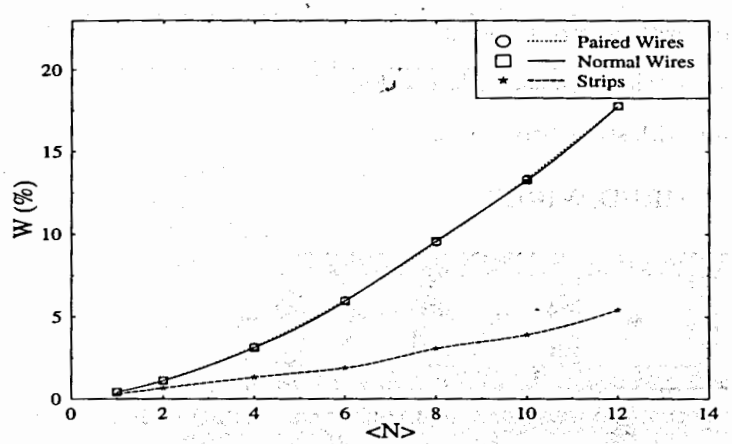

Figure 5: Probability W to identify a random direction as muon with $P_\mu = 5$ GeV for different options as a function of the average number of background particles <N>.

options with single (squares in Fig. 5) and paired wires (circles) provide an equal degree of misidentification. For <N>= 12 it is as large as $W = 17$ %. But, one should note that this result concerns the 5 GeV/c muons only, i.e. the worst case for identification. The option with strips (stars in Fig. 5) gives a gain in the identification of factor $3 - 3.5$.

To study the misidentification in case of the muon programme, we simulate the DIS of 100 GeV muons with COMGEANT code and select tracks of hadrons downstream the HCAL1. Most of these hadrons mainly can not pass through the HCAL1. However, matching the hadron tracks in front of HCAL1 with the random hits of muons from the halo in μF1 stations, it is possible to imitate a continuous track, which will be identified as a muon. The probability to identify the hadron events as muon for different options of the detector is shown in Fig. 6. It was assumed that the average number of the background muons is <N>= 12. One can see again that the options with single and paired wires have equal performance. Option with strips demonstrates a better identification. However, one could see that even for <N>= 12, which corresponds to the rate of background 300 Hz/cm^2, the

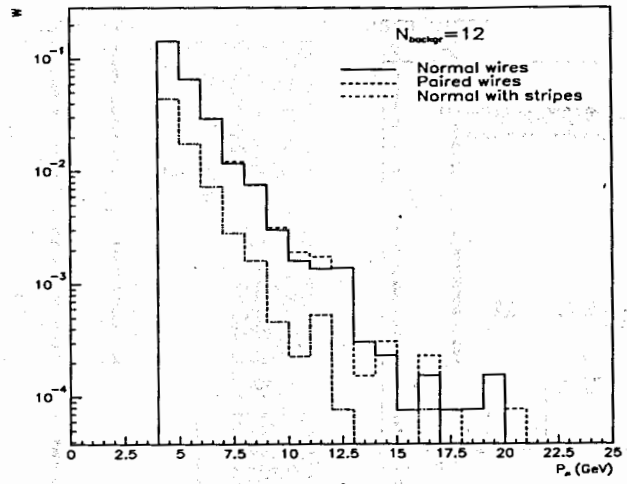

Figure 6: The probability W to identify a non-muon candidate as muon for different muon momenta P_μ.

probability to identify a track of the 10 GeV/c hadron as a muon is less than 1 % for all options. Therefore, both standard and paired options of the detector meet the physics requirements.

The similar test was done for the hadron programme. The interaction of 300 GeV proton beam with Cu target was simulated. The momentum spectrum of non-muon events is shown in Fig. 7. The dashed line shows the distribution of the events which will be misrecognized as muons. One could see that the contamination of these events is not too large.

4.2 Muon filter options

One of the ways for improving muon identification is to optimize the distance between the muon stations. Thus, increasing the distance between muon stations 1 and 2 from 15 cm (that is the proposal value) to 50 cm we can improve muon identification by factor of 2, from $M = 2.07 \pm 0.09$ % to $M = 1.09 \pm 0.08$ %. Here M is the ratio of number of non-muon candidates N_{id} identified as muons to the total number of non-muon candidates N_{cand}. Both numbers N_{id} and N_{cand} are integrals over candidate momentum spectra (with a cut P_{cand} >4 GeV/c). This estimate is for the hadron programme.

However, the space limitation in the Large Angle Spectrometer is quite severe. We would like to investigate different options of the First Muon Filter layout in order to optimize the misidentification probability.

Four options of the First Muon Filter construction have been simulated. Simu-

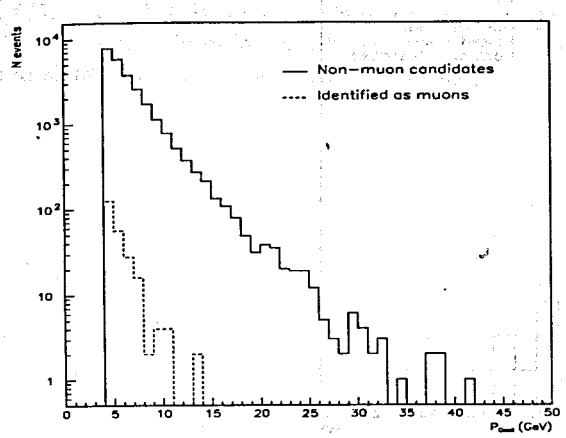

Figure 7: The momentum spectrum of non-muon events from the interaction of 300 GeV proton beam with Cu target.

lations were done for proton beam (P_p=300 GeV) and Cu target using FRITIOF event generator [3] and COMGEANT simulation code [4]. Pileup was also taken into account. Schematical representation of different options and misidentification probabilities M are shown in Fig. 8. Standard option 1, which corresponds to the proposal, gives M= 2.07 ± 0.09 %. We can obtain free space for increasing distance between the first two stations by reducing thickness of iron filter (removing one part of it). If we do so, muon misidentification probability will be $M = 2.19 \pm 0.11$ %. (option 2). If we increase the distance between stations from 15 to 50 cm, then the muon misidentification probability will be $M = 1.72 \pm 0.09$ % (option 3). Another option is to split the filter and to put the second (or third) station in a gap between two pieces of the iron filter. It gives themuon misidentification probability of $M = 1.26 \pm 0.08$ %.

A comparison of these options leads to the conclusion that the 4th option with the iron filter split into two pieces is the best one.

5 Muonic decays of D-mesons and J/ψ

To demonstrate the importance of μF1 for muon and hadron programmes, the muonic decays of D-mesons and J/ψ were studied. The decay $D_s \to \mu^- \nu$ was simulated assuming D_s production by the proton beam of 300 GeV interaction with the copper target. The momentum spectrum of muons from $D_s \to \mu^- \nu$ decays is shown in Fig. 9. Cut on the momentum of decay muons $P_\mu > 5$ GeV/c was applied

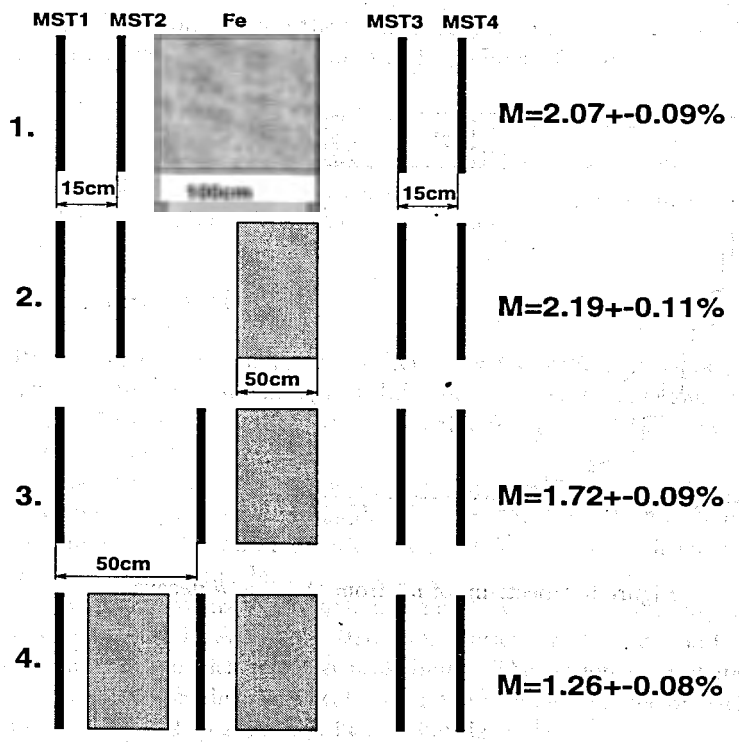

Figure 8: Schematical representation of different options of the μF1 layout and the misidentification probabilities M.

for muons emitted at large angles in μF1. For the muons emitted to the second muon filter μF2 the corresponding cut was $P_\mu > 10$ GeV/c. It turns out that 34 % of muons from $D_s \to \mu^- \nu$ decay pass through this cut and hit μF1. For the muons in μF2 the corresponding number is 32 %. So, using μF1 we can double the statistics on D_s muonic decays. Simulation of the J/ψ production by 100 GeV muons interaction with the proton target was done using AROMA2.2 generator [5].

Decay products of J/ψ and the scattered muon were detected at the first and second muon filters. The momentum spectrum of muons from $J/\psi \to \mu^+\mu^-$ decays is shown in Fig. 10. Momenta of the muons detected in the first muon filter are $5 - 50$ GeV, detected in the second muon filter - $10 - 80$ GeV. Probability P to detect 3 muons (scattered muon and muons from J/ψ decay) in case if we use the first and second muon detectors is $P = 50$ %, if we use only μF2 it is $P = 2.1$ %. Therefore the acceptance for J/ψ production is increased by 23 times using μF1. We can estimate the total number of J/ψ which could be registered in the COMPASS detector. At the 100 GeV muon energy and with a cut of $35 < \nu < 85$ *GeV* (ν is the

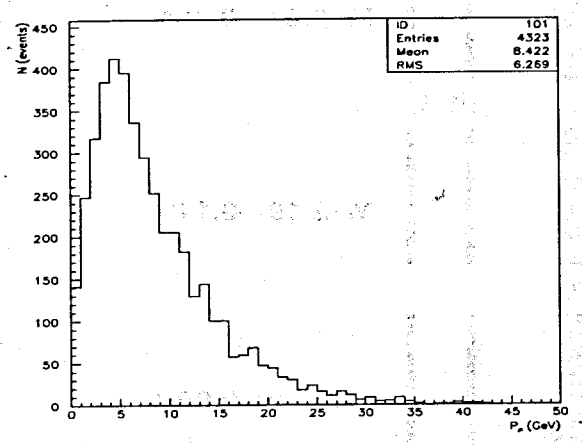

Figure 9: Spectrum of μ^- from $D_s \to \mu^- \nu$ decays.

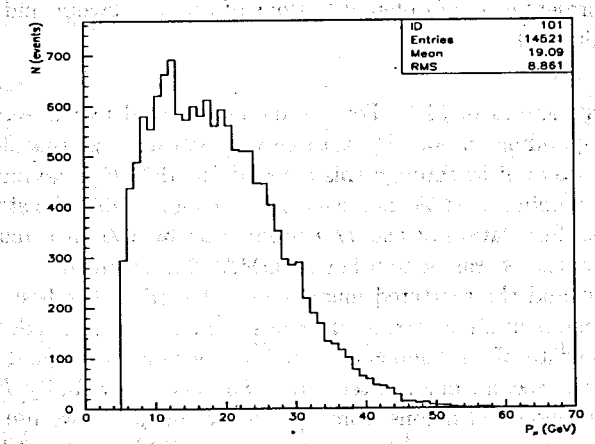

Figure 10: Spectrum of muons from $J/\psi \to \mu^+\mu^-$ decays.

energy of virtual photon) the total cross section is $\sigma(\mu^+ N \to \mu^{+'} J/\psi X) = 0.221$ nb (from AROMA). One could obtain the number of J/ψ:

$$N = \sigma \cdot L \cdot \varepsilon \cdot A \cdot Eff \cdot Br = 52 \text{ day}^{-1} \quad (1)$$

where $L = 4.3 \cdot 10^{37} \text{cm}^{-2}\text{day}^{-1}$, $\varepsilon = 0.25$ - SPS efficiency, $A = 0.5$ - three muons in acceptance, $Eff = 0.9^3$ - tracker efficiency, $Br(J/\psi \to \mu^+\mu^-)$ =0.06.

This gives 7800 J/ψ for the experimental year.

6 Conclusion

Performance of the First Muon Filter of the COMPASS spectrometer was analysed. The Monte Carlo simulation of different reactions with muons in final states was done. The construction of the individual detectors of μF1 as well as the total layout of μF1 was optimized.

The muon detection efficiency was estimated with respect to muon-trigger hodoscopes for two options of the tube construction. It was found that with the aluminium profile 0.8 mm thick we gain 10 % in overall efficiency compared to the plastic profile 1 mm thick.

Detector options with single and paired wires as well as the option with strips were studied. It was found that both options with single and paired wires give the same muon identification probability. The option with strips gives a gain of $3 - 3.5$ times in the identification for the average number of background hits per plane <N>=12 (background flux of 300 Hz/cm^2).

Different options of First Muon Filter layout were studied in order to optimize the misidentification probability and the detector space. It was found that the option with the iron filter split into two pieces is the best one.

The authors are grateful to M. I. Gostkin, N. P. Kravchuk, S. Yu. Porokhovoy and S. I. Merzlyakov for fruitful discussions.

References

[1] The COMPASS Collaboration, Proposal, CERN/SPSLC 96-14.

[2] G. Alexeev *et al.*, DØ Note # 3366, FNAL, December 1997, E. Iarocci, Nucl. Instr. and Meth. **217**, 30 (1983).

[3] B. Nillson-Almqvist and E. Stenlund, Comp. Phys. Comm. **43**, 387 (1987), H. Pi, Comp. Phys. Comm. **71**, 173 (1992).

[4] COMGEANT Home Page,
http://wwwcompass.cern.ch/compass/sp/software/simul/comgeant/

[5] G. Ingelman, J. Rathsman, G. A. Schuler, AROMA 2.2, program manual, DESY 96-058.

Received by Publishing Department
on June 30, 1998.